Neurotherapeutics 21 (2024) e00312

Contents lists available at ScienceDirect

Neurotherapeutics

journal homepage: www.sciencedirect.com/journal/neurotherapeutics

Original Article

Recombinant soluble form of receptor for advanced glycation end products ameliorates microcirculation impairment and neuroinflammation after subarachnoid hemorrhage

Ling-Yu Yang [a], Sung-Chun Tang [b], Jing-Er Lee [c], Yong-Ren Chen [d,g], Yi-Tzu Chen [a], Kuo-Wei Chen [a], Sung-Tsang Hsieh [e,f], Kuo-Chuan Wang [a,*]

[a] Division of Neurosurgery, Department of Surgery, National Taiwan University Hospital and National Taiwan University College of Medicine, Taipei, Taiwan
[b] Department of Neurology, National Taiwan University Hospital and National Taiwan University College of Medicine, Taipei, Taiwan
[c] Department of Neurology, Taipei Medical University-Wan Fang Hospital, Taipei, Taiwan
[d] Non-invasive Cancer Therapy Research Institute, Taipei, Taiwan
[e] Department of Neurology, National Taiwan University Hospital, Taipei, Taiwan
[f] Department of Anatomy and Cell Biology, National Taiwan University College of Medicine, Taipei, Taiwan
[g] Division of Neurosurgery, Department of Surgery, National Taiwan University Hospital Jin-Shan Branch, New Taipei City, Taiwan

ARTICLE INFO

Keywords:
Aneurysmal subarachnoid hemorrhage
Soluble form of receptor for advanced glycation end products (sRAGE)
Microcirculation impairment
Brain edema
Endothelial dysfunction
Neuroinflammation

ABSTRACT

Impaired cerebral microcirculation after subarachnoid hemorrhage (SAH) has been shown to be related to delayed ischemic neurological deficits (DIND). We previously demonstrated the involvement of the receptor for advanced glycation end products (RAGE) in the pathogenesis of SAH related neuronal death. In the present study, we aimed to investigate the therapeutic effects of a recombinant soluble form of RAGE (sRAGE) on microcirculation impairment following SAH. Intrathecal injection of autologous blood in rats, mixed primary astrocyte and microglia cultures exposed to hemolysates and endothelial cells (ECs) from human brain microvascular exposed to glia-conditioned medium or SAH patient's CSF were used as experimental SAH models in *vivo* and in *vitro*. The results indicated that intrathecal administration of recombinant sRAGE significantly ameliorated the vasoconstriction of cortical arterioles and associated perfusion impairment, brain edema, reduced cell death, endothelial dysfunction, and improved motor performance at 24 and 48 h after SAH induction in rats. The in vitro results further showed that recombinant sRAGE significantly reduced astrocyte swelling and microglia activation, in parallel with decreased mRNA expression levels of pro-inflammatory cytokines including interleukin-6 (IL-6) and interleukin-1β (IL-1β) in *vitro*. Moreover, the in vitro model of SAH-induced p-eNOS and eNOS suppression, along with stress fiber formation in brain microvascular ECs, was effectively reversed by sRAGE treatment and led to a decrease in cleaved-caspase 3 expression. In summary, recombinant sRAGE effectively lessened microcirculation impairment and vascular injury after SAH via the mechanism of anti-inflammation, which may provide a potential therapeutic strategy for SAH.

Introduction

Aneurysmal subarachnoid hemorrhage (SAH) carries significant morbidity and mortality with one-third of survivors suffering long-term physical, neurocognitive, or psychological impairments [1,2]. The majority of deaths following SAH occur within two days of the onset of bleeding [3]. Moreover, early brain injury that occur within 72 h after SAH has been considered to contribute to poor outcomes. Products of red blood cell lysis in the subarachnoid space could cause excessive neuroinflammation during early brain injury, which contributes to disruption of the blood–brain barrier (BBB), cerebral edema, vasospasm and delayed ischemic neurological deficits (DINDs) [4]. Several studies suggested that the main cause of DINDs may arise from the constriction of microvessels on the brain surface rather than large cerebral arteries [5,6]. Evidence suggests that cerebral microcirculation plays a crucial role in the proper functioning of the brain as it supplies oxygen and glucose to the highly metabolically active neurons. The microcirculation consists of a complex network of capillaries, pre-capillary arterioles and venules that

* Corresponding author.
E-mail address: wang081466@yahoo.com.tw (K.-C. Wang).

https://doi.org/10.1016/j.neurot.2023.e00312
Received 30 November 2023; Received in revised form 12 December 2023; Accepted 15 December 2023

penetrate the brain parenchymal to adequately supply the regional circulation, and are supported by the astrocyte foot processes [7,8]. Disruptions in cerebral microcirculation can lead to reduced cerebral blood flow and have detrimental effects on brain function, and have been associated with various neurological disorders, such as stroke, traumatic brain injury, and dementia [9,10]. However, the pathophysiological mechanism of post SAH microcirculational change and its association with the development of DINDs have not been well investigated.

The receptor for advanced glycation end products (RAGE) is a cell surface receptor that is found in neurons, glial cells and endothelial cells of the central nervous system (CNS) and has the ability to interact with a variety of ligands, including high-mobility group box 1 (HMGB1), S100 proteins, advanced glycation end products (AGEs), and amyloid β-peptide [11,12]. There is growing evidence showing that HMGB1-RAGE signaling plays an integral role in the development and progression of endothelial dysfunction and brain edema, which may further lead to vascular damage and worsening of neurological function following ischemic or hemorrhagic brain damage [13–15]. In addition, the inhibition of RAGE signaling by HMGB1 or RAGE antibodies protects against stroke-induced apoptosis, astrocyte swelling and reduced infarct volume according to some basic research [16–19]. A soluble form of RAGE (sRAGE) that is lacking the transmembrane and intracellular domains has been found to act as an inhibitor of RAGE by competing with canonical ligands, such as HMGB1, leading to the suppression of RAGE/NF-κB signaling cascades [20]. The potential therapeutic utility of sRAGE has attracted attention in terms of the prevention of RAGE-mediated disease pathogenesis. We and others previously reported that treatment with recombinant sRAGE attenuated neuroinflammation and provided marked protection against SAH-induced neuronal death [18,21]. However, the therapeutic effect of sRAGE in protection against SAH-induced cerebral microcirculation impairment remains poorly understood.

Recently, we have successfully established a rat model of SAH and demonstrated the impaired microcirculation, as indicated by a significantly diffuse constriction of cortical arterioles, decreased blood flow and partial pressure of oxygen on the brain surface [21,22]. In the present study, we aimed to evaluate the therapeutic effects and mechanisms of sRAGE on post SAH microcirculation impairment and endothelial dysfunction in an experimental SAH rat model, a mixed primary astrocyte-microglia co-cultures and endothelial cells from human brain microvascular SAH in vitro models.

Methods

This study included the performance of animal experiments and obtaining cerebrospinal fluid (CSF) from human subjects was approved by the Utilization Committee and the National Taiwan University Institutional Laboratory Animal Care Committee (IACUC No. 20201255) and the Institutional Review Board of National Taiwan University Hospital, Taipei, Taiwan (IRB No. 201301042RINB). Animal studies are reported in compliance with the ARRIVE guidelines [23].

Animal model of SAH

SAH was induced in Male Wistar rats (7 weeks old; weighing 250–300 g) by intrathecal injection of freshly autologous blood, as described in previous studies [21,22,24]. The animals were randomized into 5 groups: (i) Control, (ii) SAH24h + Veh, (iii) SAH24h + sRAGE, (iv) SAH48h + Veh, (v) SAH48h + sRAGE. Surgeries and all biochemical/histological analyses were performed by investigators blinded to treatment allocation through the entire duration of the study. After anesthetization with 2.5 % isoflurane with 70 % nitrous oxide and 27.5 % oxygen, the rat's femoral arterial pressure was monitored using an RFT Biomonitor, VEB (Messgeraetewerk, Germany). A small incision was made in the suboccipital muscles to expose the cisterna magna, then the SAH model was induced by injecting 0.3 ml of fresh autologous blood into the cisterna magna. After injecting the blood, the rat's head was placed in a 20-degree head-down position over a 5-min period to prevent reflux of blood from the injection site. The SAH rats randomly received vehicle (saline) or recombinant sRAGE (AVISCERA Bioscience, USA) at the time of SAH induction (0.l ug/rat was used for treatment based on our previous study [21], intrathecal injection). Control animals received anesthesia and small incision but no SAH induction. After the wound area was sutured, body temperature was monitored and maintained at 37.0 ± 0.5 °C using a heated pad over a period of 4 h.

Microvasculature density

Microvasculature density at the brain surface was performed at 24 or 48 h after SAH induction as described previously [22,24]. Briefly, the animals were anesthetized and the dura mater removed after a 3 × 3 mm^2 craniotomy at the left frontal suture. High-resolution (752 × 582 pixels) microscopy was performed using a CAM1 Capillary Anemometer (KK Technology, England) connected to a charge-coupled device (CCD) and a computer. The field of view was 684 × 437 μm^2, and the image was magnified to an overall magnification of 0.91 μm/pixel. To quantify the vessel diameter, we identified the 1–2 main arterioles in the craniotomy site and then took photographs along the primary arterioles (pa), followed by the secondary arterioles (sa), and finally the terminal arterioles (ta) according to the branch order. We recorded more than 10 photographs at the craniotomy site and measured the diameters of the sampled pa, sa and ta individually in each animal group.

Measurement of regional brain blood flow and brain tissue oxygen tension ($PbtO_2$)

Brain regional blood flow and $PbtO_2$ were measured with the OxyLite 2000E and OxyFLO 2000E detectors (Oxford Optronic Ltd, England) using a fluorescence quenching technique. After the rat and probe were fixed to the stereotactic apparatus, the detection fibre-optic probe was positioned 2 mm deep from the brain surface. Continuous monitoring of perfusion parameters was conducted on the cortical surface to record $PbtO_2$, blood flow, and temperature in the same micro-region for 30 min.

Transmission electron microscopy (TEM)

To examine the microcirculation impairment, TEM was performed on cortical tissue taken 24 or 48 h after SAH induction. Brain slices were pre-fixed in PBS with 2.5 % glutaraldehyde and post-fixed with 2 % osmium tetroxide for 1 h. After dehydration in a graded series of ethanol, ultrathin sections were cut and placed on a copper grid and then lightly stained with lead citrate. The specimens were submitted to high-resolution transmission electron microscopy (JEOL JEM-1400, Japan) at 80 kV.

Brain water content

After inducing SAH, rats were sacrificed at either 24 or 48 h. Subsequently, their brains were swiftly removed, and we only peeled off and isolate the cortical tissue. This cortical tissue was then promptly collected and weighed (wet weight). Next, the cortical tissue was subjected to a 3-day drying process in an 80 °C oven to ensure complete desiccation. Finally, the dried tissue was weighed again to obtain its dry weight. The brain water content was calculated as (wet weight − dry weight)/wet weight x 100 % [25].

Rotarod test

The rotarod test is widely used to assess motor performance in rats [26]. The test was performed as previously described [27]. Before SAH surgery, each rat was placed on the instrument (Panlab Rota Rod, Havard Apparatus) at a speed of 4 rpm for three consecutive days, three sessions per day for 5 min. At 24 or 48 h after SAH induction, the latency to fall of

each rat was recorded at the speed of 4–40 rpm, in 600 s, during a 5-min testing period.

Enzyme-linked immunosorbent assay (ELISA)

Cerebrospinal fluid (CSF) was harvested via lumbar puncture at 24 or 48 h after SAH induction. CSF samples were centrifuged at 900 g for 20 min at 4 °C and then divided into suitable aliquots. The supernatant were be collected and immediately stored at −80 °C. The samples were assayed in duplicate using an endothelin-1 (ET-1) assay kit (ADI-900-020A, Enzo Life Sciences), nitric oxide production asymmetric dimethylarginine (ADMA) assay kit (KR3001, ImmunDiagnostik) or dimethylarginine dimethylaminohydrolase 2 (DDAH 2) assay kit (E02D0012, BlueGene) according to the manufacturer's guidelines.

Immunohistochemistry

Serial coronal brain sections (10 μm) were used for single/double-fluorescent immunohistochemistry staining and TUNEL staining. The brain sections were deparaffinized and rehydrated in PBS. For the TUNEL assay, sections were blocked to nonspecific antibody binding with PBS containing 0.1 % Triton-X 100 and 10 % normal goat serum for 60 min followed by incubation overnight using a TdT FragEL DNA fragmentation detection kit (Merck Millipore, Germany) as per the manufacturer's instructions. For single/double-fluorescent immunohistochemistry staining, sections were blocked and subsequently immunostained with rabbit anti-Iba1 (019-19741, Wako) and rabbit anti-GFAP (ab7260, Abcam), mouse anti-glucose transporter 1 (GLUT1, ab40084, Abcam) and rabbit anti-fibrinogen (A0080, DAKO) overnight at 4 °C. Thereafter, immunolabeling was performed using Alexa Fluor 488- and 594-conjugated secondary antibodies (Invitrogen) at room temperature for 30 min and counterstaining with DAPI. Quantification of the number of Iba1-positive cells or the percentage of GLUT1/fibrinogen-positive cells was performed based on five randomly selected 20× magnification. Cell numbers were expressed as counts/mm^2. To quantify GFAP levels, the mean fluorescent intensity (MFI) of GFAP was determined by measuring the mean gray value in five fields per sample at a 20× magnification. All images were examined under a Nikon Eclipse Ti2 fluorescence microscope attached to a digital camera and analyzed using ImageJ software.

Primary rat cortical astrocyte/microglia co-cultures

Primary astrocyte/microglia co-cultures were isolated from the cerebral cortex of 1-day-old neonatal Wistar rats as previously described [27,28]. Cortical tissues were collected from pups and placed in ice-cold Ca/Mg free-HBSS. After removal of the meninges, cells were dissociated by pipetting up and centrifuged (1500 rpm) at 4 °C for 5 min. The cell pellet was transferred into 10-cm culture dish at 5×10^5 cells/ml (10 ml/dish) in Dulbecco's Modified Eagle's Medium (DMEM; Corning, NY, USA) with 10 % FBS, 1 % penicillin and 0.25 % gentamycin and then incubated at 37 °C with 5 % CO2. When cells grew to confluence (10–12 d), the astrocytes/microglia were subsequently detached using trypsin and then randomly assigned to different treatments.

Preparation of hemolysate

To mimic an in vitro model of SAH, the mixed astrocyte/microglia were subjected to hemolysate which was obtained from lysis of red blood cells. Hemolysate was prepared by a rapid freeze-thaw method and a concentration of hemolysate of 1 mg/ml was used for treatment based on previous SAH studies [27,29]. Briefly, blood samples were collected in tubes containing heparin via cardiac puncture in rats and centrifuged at 2500×*g* for 15 min at 4 °C. After discarding the supernatant, the red blood cells were re-suspended in an equal volume of sterile distilled water and then frozen at −80 °C for 30 min. Frozen red cells were thawed in a 39 °C bath and then centrifuged at 14,000×*g* for 30 min at 4 °C. The supernatant containing hemolysate was collected and stored at −80 °C. The mixed astrocyte/microglia co-cultures were randomly assigned into 3 groups: (i) PBS-treated control group; (ii) hemolysate (1 mg/ml) + Veh (PBS) treatment group; (iii) hemolysate (1 mg/ml) with sRAGE (50 ng/ml) treatment group. All cells were incubated for 24 h at 37 °C, 5 % CO_2.

Collection of CSF from SAH patients

CSF collection from SAH patients has been previously documented [21]. We selected CSF from SAH patients with an unfavorable outcome to serve as a SAH in vitro model. Intrathecal CSF was collected by lumbar puncture on the seventh day following SAH according to our previously established protocol [22]. The CSF samples were immediately centrifuged at 900×*g* at 4 °C for 20 min before being divided into suitable aliquots and rapidly frozen at – 80 °C within 30 min. Written informed consent was obtained from all patients or their legal representatives for this study.

Human primary brain microvascular endothelial cells

Culture of human brain microvascular endothelial cells (HBMECs) were obtained from Cell Systems (Cat# ACBRI376). HBMECs were routinely grown in Complete Classic Medium (4Z0-500, Cell Systems, USA), supplemented with CultureBoost™ (4CB-500, Cell Systems, USA), and 1 % antibiotics (penicillin-streptomycin). All cells (passages 5–12) were grown on Attachment Factor (4Z0-210, Cell Systems, USA)-coated 6 cm dishes and maintained in a humidified incubator with 5 % CO_2/95 % air at 37 °C.

For experimental purposes, cells were randomly subjected to into 5 groups: (i) PBS-treated control group; (ii) glia-conditioned media (changing the conditioned medium by 25 %, conditioned media was acquired following a 24 h incubation period of primary mixed astrocyte/microglia co-cultured media with 1 mg/ml hemolysate) with Veh (PBS) treatment group or (iii) sRAGE (50 ng/ml) treatment group; (iv) SAH patient's CSF (10 %) with Veh (PBS) or (v) sRAGE (50 ng/ml) treatment group. All cells were incubated for 12 h at 37 °C, 5 % CO_2. The selection of concentrations and treatment duration was informed by prior utilization in scientific literature [27,30].

Immunocytochemistry (ICC)

Primary mixed astrocytes/microglia co-cultures or HBMECs were fixed with 4 % paraformaldehyde for 20 min. After washing with PBS, cells were permeabilized and blocked in 3 % bovine serum albumin with 0.1 % Triton X-100 for 1 h at room temperature. Then, the glia cells were incubated with primary antibodies for mouse monoclonal CD11b (OX-42, ab1211, Abcam) and rabbit polyclonal GFAP (ab7260, Abcam) at 4 °C overnight. After washing with PBS, cells were incubated with Alexa Fluor 488- and 594-conjugated secondary antibodies (Invitrogen, USA) at room temperature for 30 min and counterstained with DAPI. The HBMECs were incubated with p-eNOS (Ser1177, MA5-14957, Invitrogen) at 4 °C overnight. Appropriate secondary antibodies, conjugated to Alexa-Fluor-594 and phalloidin-FITC (F432, Molecular Probes) was used to visualize the F-actin. The staining process was carried out at room temperature for 30 min, followed by counterstaining with DAPI.

Quantification of the numbers of OX42-positive cells was performed based on five randomly selected magnification fields. All images were examined under a Nikon Eclipse Ti2 fluorescence microscope attached to a digital camera and analyzed using ImageJ.

Measurement of the cell perimeter

Changes in astrocytic cell volume in the astrocyte/microglia co-culture were determined using the perimeter method according to previously studies [31,32]. The perimeter was calculated using Image J software after GFAP immunofluorescence staining. In each 200 × magnification field of view, 5 fields in every group, 10 cells were

randomly selected for calculation. The average value of five fields was taken as the cell perimeter of each group.

Western blot analysis

Proteins from cortical tissue or HBMECs were harvested at 24 h after SAH induction or at 12 h after treatment duration, respectively. The samples were lysed in protein extraction buffer (iNtRON Biotechnology, Korea) supplemented with protease inhibitors (Roche, Diagnostics, USA). Then, lysed sample was centrifuged at 13,000 g for 10 min at 4 °C, and the supernatant was collected and stored at − 80 °C until use. Proteins were subjected to electrophoresis on 12 % polyacrylamide gels (Bio-Rad) and then transferred to a nitrocellulose membrane (BioRad, USA). Membranes were blocked with 5 % non-fat milk for 1 h at room temperature. After blocking, membranes were incubated overnight at 4 °C with primary antibodies against cleaved-caspase 3 (9661, Cell Signaling Technology), p-eNOS (Ser1177, MA5-14957, Invitrogen), eNOS (07-520, EMD Millipore) and GAPDH (MA515738, Thermo Fisher). After incubation with goat polycolonal anti-rabbit IgG (Gene-Tex) and goat polycolonal anti-mouse IgG (GeneTex) for 1 h at room temperature, membranes were visualized using enhanced chemiluminescent (ECL) detection reagents for 5 min. We were performed consistently procedures across all gels to minimize variability. The expression levels of proteins were normalized to GAPDH on each gel. Several exposure times were analyzed to confirm the linearity of the band intensities. To standardize and quantify the immunoblots, we used the UVP BioSpectrum 810 system (Upland, USA) and ImageJ software.

Quantitative real-time PCR

Total RNA were purified from cortical tissue or primary cultured astrocyte/microglia using TRIzol reagent (Invitrogen, USA) as per the manufacturer's instructions. Total RNA (2 μg) was reverse-transcribed to cDNA using M-MLV reverse transcriptase (Promega Corporation, USA). Real-time PCR was carried out at 98 °C for 2 min, 98 °C for 2 ses, 58 °C for 5 s, followed by 40 cycles using a Kapa SYBR Fast qPCR Kit (Kapa Biosystems, USA) and primers for IL-6, 5′- TGGAGTTCCGTTTCTACCTGGA -3’ (forward); 5′- GAGCATTGGAAGTTGGGGTAGG -3′ (reverse); IL-1β, 5′- GCACTGCAGGCTTCGAGATG -3’ (forward) and 5′- AGGCCACAGGGAT TTTGTCG -3’ (reverse); Ppib, 5′- GCACGTGGTTTTCGGCAAAG -3’ (forward) and 5′- TTGGCAATGGCAAAGGGTTT -3’ (reverse). Amplification and detection were performed using a 7900 Real-Time PCR System (Applied Biosystems, USA). The relative mRNA levels were normalized to the housekeeping protein Ppib and calculated using the ΔΔCt method. All values were expressed as fold changes compared with control samples.

Statistical analysis

For in vivo experiments, data were obtained from 5 rats in each group. For in vitro experiments, data were obtained from at least 3 independent experiments. All statistical data are expressed as the mean ± SD. Data and bar graph displays were analyzed using using GraphPad Prism 7.0 software (GraphPad Software, USA). Based on the Shapiro–Wilk normality test, comparisons between several groups were performed by one-way analysis of variance (ANOVA) followed by the Post Hoc Test (Tukey's multiple comparisons test) for normally distributed data, and with the Kruskal–Wallis variance analysis test for non-normally distributed data. Statistical significance was defined as $P < 0.05$.

Results

Intrathecal administration of recombinant sRAGE ameliorated the post SAH vasoconstriction of cortical arterioles and associated perfusion impairment

To investigate the treatment effects of recombinant sRAGE on cortical surface microcirculation alterations, we performed a 3 × 3 craniotomy window at 24 or 48 h after SAH. Vasculatures including the main arterioles and venules on the brain surface were noted by videoscope (Fig. 1A). As compared with the controls (Fig. 1B, B1&2), markedly diffuse vasoconstriction was observed in the SAH24h + Veh and SAH48h + Veh groups (Fig. 1B, B3&4, B7&8). Reversibility of SAH-associated vasoconstriction was noted at 24 and 48 h in the recombinant sRAGE treatment group (Fig. 1B, B5&6, B9&10). After quantifying the diameters of cortical arterioles, which were divided into primary arterioles (pa), secondary arterioles (sa), and terminal arterioles (ta). Markedly vasoconstriction was observed over the brain surface 24 h after SAH induction when compared to sa and ta in the control group, but no vasoconstriction was observed at the 48 h post-SAH. It is noteworthy that the diameters of the sa and ta significantly increased as time from 24 to 48 h after SAH. In addtion, the sRAGE treatment group had significantly larger diameters of pa, sa and ta at 24 h than the vehicle group, while only the diameters of ta in the sRAGE treatment group was larger than the vehicle group at 48 h (Fig. 1C). Next, in order to further investigate the cerebral perfusion assessment, a detection fibre-optic probe was performed at a depth of 2 mm from the cortex to measure the cerebral blood flow and brain tissue oxygen partial pressure ($PbtO_2$) (Fig. 2A). Notably, despite the increase in arteriole diameters at brain surface, the decrease in cerebral blood flow and $PbtO_2$ induced by SAH at 24 h did not show improvement at 48 h in the animals (Fig. 2B&C). Treatment with sRAGE significantly improved the regional blood flow and tissue oxygen pressure as compared with the vehicle group at both 24 and 48 h post-SAH, respectively (Fig. 2B&C). During the measurements, blood pressure did not differ significantly between groups, suggesting that the positive effect of sRAGE treatment in improving cerebral perfusion was not related to the change in blood pressure (Fig. 2D).

Recombinant sRAGE mitigated astrocyte swelling-mediated cerebral microcirculation impairment and restored the lumen of the capillary endothelium in SAH rats

In light of the paradox between the diameters of brain surface arteriole and the blood flow/tissue oxygen pressure beneath brain surface, we further used electron microscopy (EM) to observe the structure of the astrocytes and capillaries at around 2 mm from the cortical surface (Fig. 3A). In the control group, the astrocyte end-feet were thin and surround the entire capillaries. At 24 h after SAH, the astrocyte end-feet were swollen, and compressed the capillary lumen in the vehicle group, and the phenomenon was more prominent at 48 h. Administration of recombinant sRAGE remarkably mitigated the swelling of astrocyte end-feet and restored the capillary lumen at both 24 and 48 h post-SAH. Moreover, we observed marked increase in cortical water content as compared to the control at both 24 and 48 h after induction of SAH group (Fig. 3B; $p < 0.01$ vs. SAH24h + Veh; $p < 0.001$ vs. SAH48h + Veh). Notably, sRAGE treatment significantly attenuated SAH-mediated increases in cortical water content (Fig. 3B; $p < 0.05$ vs. SAH24h + Veh; $p < 0.001$ vs. SAH48h + Veh).

Recombinant sRAGE treatment significantly inhibited activation of astrocytes, microglia and inflammation induced by SAH

Next, we measured astrocyte and microglia activation in the cortical reagion across the five groups (Fig. 4A). As shown in Fig. 4B–E, there were significant increases in astrocyte (the intensity of GFAP) and microglia (Iba1-positive) expression between the control and SAH24h + Veh/SAH48h + Veh groups. However, sRAGE treatment significantly attenuated the astrocyte and microglia activation induced by SAH (Fig. 4D and E). To investigate the roles of sRAGE in regulating microglia-mediated pro-inflammation response following SAH, we further examined the mRNA expressions of pro-inflammation molecules IL-6 and IL-1β in the cortex at 24 and 48 h after SAH. IL-6 and IL-1β were both significantly elevated within the SAH24h + Veh group as compared with the control group, but not in SAH48h + Veh group (Fig. 4F). In contrast,

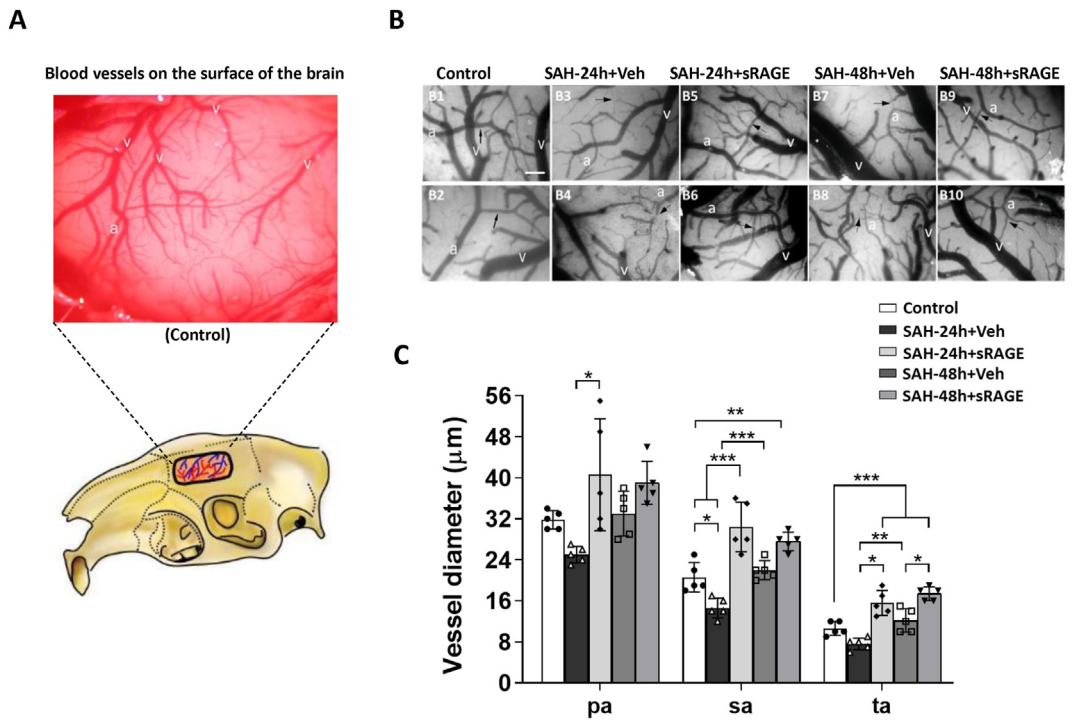

Fig. 1. Administration of sRAGE reduced vasoconstriction of small arterioles on the brain surface after SAH. (A) A 3 × 3 mm cranial window was created using a motorized drill and the left skull was exposed (lower panel). After removing dura, the blood vessels on the surface of the brain was observed (upper panel). (B) The vasculature images under capillary videoscopy were captured from the (B1&2) control, (B3&4) SAH24h + Veh, (B5&6) SAH24h + sRAGE, (B7&8) SAH48h + Veh and (B9&10) SAH48h + sRAGE groups (2 animals per group). The vasculature, including the artery (a) and vein (v), was clearly seen on the brain surface. (C) Quantitation of the arteriole diameters of primary (pa), secondary (sa) and terminal (ta) arterioles from 5 groups. Data are expressed as means ± SD. Scale bar = 100 μm $^{*}P < 0.05$, $^{**}P < 0.01$, $^{***}P < 0.001$ ($n = 5$ in each group).

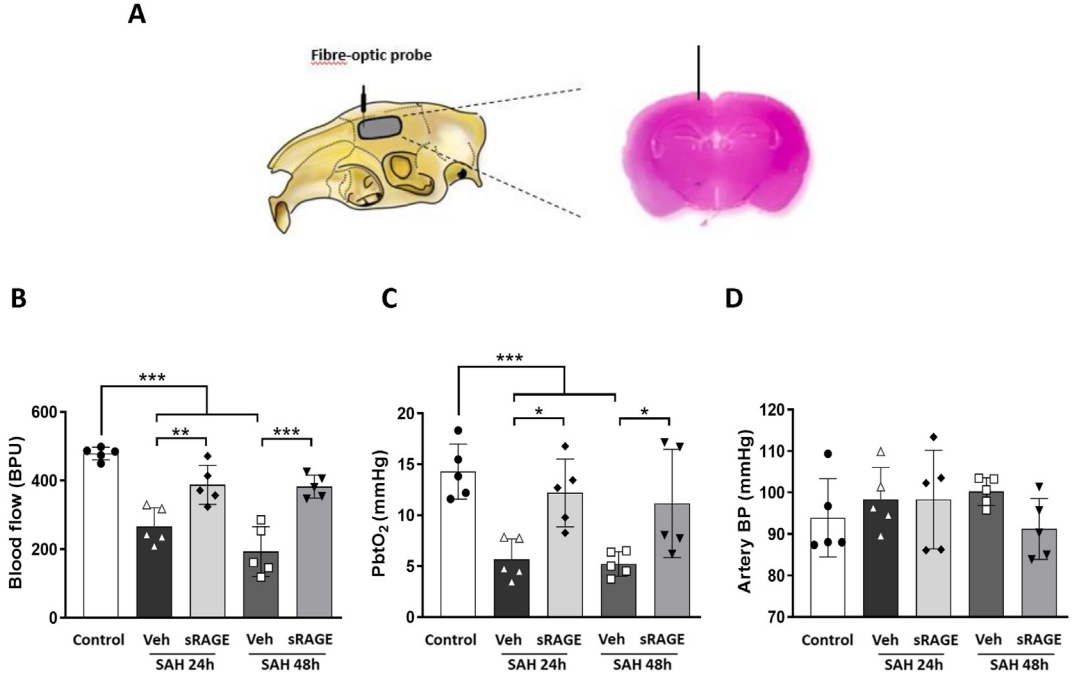

Fig. 2. Administration of sRAGE reduced microcirculation impairment after SAH. (A) The microcirculation measurement was performed using a fibre-optic probe with a parameter of 2 mm below the dura. Scheme and photomicrograph presenting the section of the brain with probe positioning in the right panel. (B) Regional blood flow, (C) partial pressure of oxygen ($PbtO_2$) and (D) arterial blood pressure were recorded at a 2-mm depth from the cortex in all groups at 24 or 48 h post-SAH. After quantitation, the impaired blood flow and $PbtO_2$ were significantly increased in the sRAGE group as compared with the SAH24h + Veh and SAH48h + Veh groups. Data are expressed as means ± SD.$^{*}P < 0.05$, $^{**}P < 0.01$, $^{***}P < 0.001$ ($n = 5$ in each group).

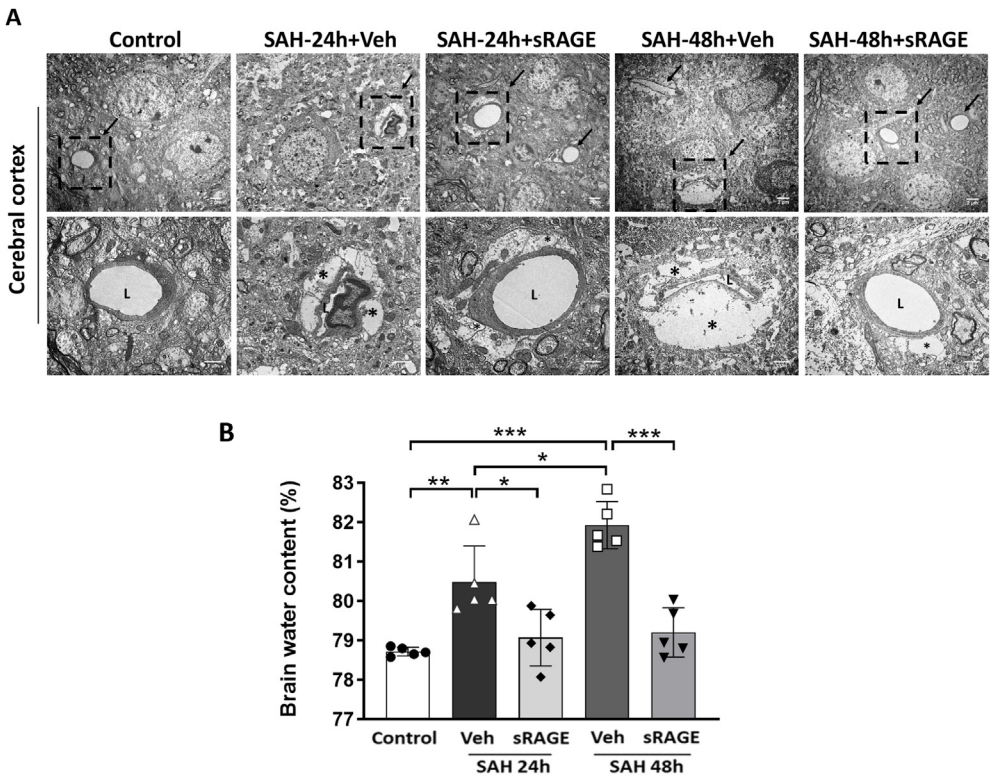

Fig. 3. Administration of sRAGE attenuated SAH-induced brain edema and restored the compressed microvessels. (A) Electron micrograph findings in the cerebral cortex from 5 groups. The arrows point to the microvessels in representative electron micrographs in the upper panel (bar = 2 μm). The lower panel is an enlargement of boxed areas in the upper panel (bar = 1 μm). The lumen of the microvessel is marked L and the astrocyte end-feet are marked with asterisks (*). Remarkably swollen end-feet compressed the microvessels in the SAH24h + Veh and SAH48h + Veh groups, whereas sRAGE administration attenuated the astrocyte swelling and restored the compressed microvessels. (B) The sRAGE administration significantly reduced the brain water content in the cortex region at 24 or 48 h after SAH. Data are expressed as means ± SD.*$P < 0.05$, **$P < 0.01$, ***$P < 0.001$ ($n = 5$ in each group).

treatment with sRAGE significantly decreased the mRNA expression levels of IL-6 and IL-1β as compared with the SAH24h + Veh group (Fig. 4F).

Recombinant sRAGE treatment reduced the thrombotic vessels, the levels of ET-1, and ADMA and increased the levels of DDAH2 in the CSF in SAH rats

Double-labeling immunofluorescence of fibrinogen (a thrombotic marker) and GLUT1 (an endothelium maker) was used to evaluate the proportion of thrombosed vessels in the cortical region. The results indicated that the amount of positive fibrinogen staining was markedly increased in the vehicle group at both 24 and 48 h after SAH, but not in the sRAGE treatment group at 24 and 48 h as compared with the control group (Fig. 5A; $p < 0.001$). Intrathecal injection of recombinant sRAGE significantly decreased the proportion of thrombosed vessels after SAH (Fig. 5B; $p < 0.001$). In addition, it has been well-recognized that increased ET-1 and ADMA levels, as well as a decreased DDAH2 level, in the CSF are hallmarks of endothelial dysfunction after brain insult [33–36]. As shown in Fig. 6, SAH significantly increased the levels of ET-1 and ADMA, in parallel with a decreased level of DDAH2, in the CSF at 24 and 48 h after SAH (Fig. 6A–C). Intrathecal administration of recombinant sRAGE significantly reduced the ET-1 and ADMA levels and increased the DDAH2 level at 48 h after SAH as compared with the vehicle group (Fig. 6A–C).

Recombinant sRAGE treatment prevented cell death and improved motor performance in SAH rats

TUNEL staining and Western blot analysis were performed to assess the apoptotic cells and the expression of cleaved caspase-3 in the cortical region. The results indicated that TUNEL-positive cells were increased in the SAH + vehicle group at both 24 and 48 h as compared with the control, while TUNEL-positive cells were markedly decreased in the sRAGE treatment group as compared with the SAH + Veh group at 24 and 48 h (Fig. 7A). The WB data showed that the cleaved caspase-3 level was significantly increased in the SAH24h/48 h + Veh groups, but not the SAH24h/48 h + sRAGE groups, as compared with the control (Fig. 7B). In the rotarod test, SAH induced functional impairment at 24 and 48 h, as indicated by a significant decrease in the latency to fall time, while sRAGE treatment reversed the reduction in time at 24 and 48 h post-SAH (Fig. 7C).

Recombinant sRAGE reduced microglia activation, astrocyte swelling, and pro-inflammatory cytokine mRNA levels in primary co-cultures of astrocyte and microglia exposed to hemolysate

To examine whether blood lysate directly influences the inflammatory response and astrocyte swelling post SAH, we applied hemolysate to co-cultures of astrocytes and microglia. After exposure to hemolysate for 24 h, the number of $OX42^+$ microglia cells increased significantly (Fig. 8A&B; $P < 0.001$ vs. Control), while treatment with sRAGE effectively reduced the number of $OX42^+$ microglia cells (Fig. 8B; $P < 0.001$ vs. Veh). Astrocyte swelling was estimated by measuring the $GFAP^+$ cell perimeter to reference the level of cell volume change. Treatment with sRAGE significantly reversed the hemolysate-induced elevation of the $GFAP^+$ cell perimeter (Fig. 8C; $P < 0.001$ vs. Veh). We also measured the pro-inflammatory cytokine mRNA expressions of IL-6 and IL-1β in co-cultures of astrocytes and microglia. IL-6 and IL-1β were significantly increased in the hemolysate + Veh group, but not in the hemolsate + sRAGE group as compared with the control group (Fig. 8D).

Recombinant sRAGE attenuates vascular injury and NO production impairment in brain microvessels exposed to glia-conditioned medium or SAH patient's CSF

To confirm the effect of sRAGE on SAH-induced vascular injury and nitric oxide (NO) production impairment, SAH patient's CSF (10 %) or conditioned medium (25 %) from primary mixed glia culture treated with hemolysate were used to induce vascular endothelial cell injury in HBMECs. To investigate the potential impairment of NO synthesis in HBMECs by SAH patient's CSF, we conducted Western blot analyses for endothelial nitric oxide synthase (eNOS) and phosphorylation of eNOS

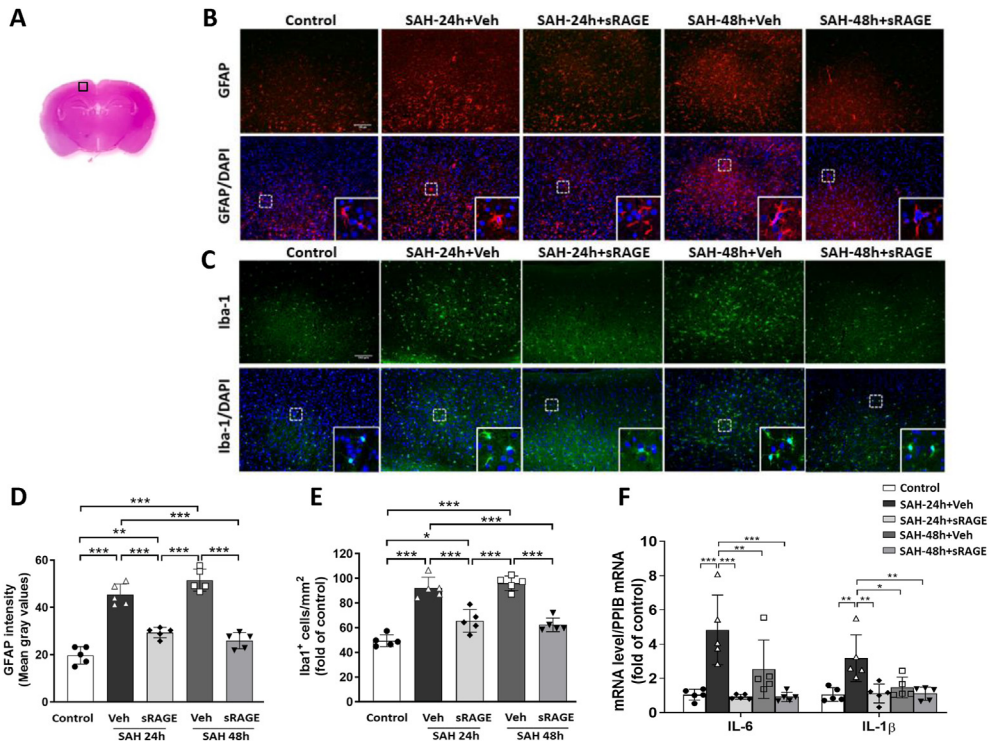

Fig. 4. Administration of sRAGE relieved astrocyte and microglia activation in the cortical region. (A) The representative HE-stained coronal section showing the area as indicated by the cortex region (black square box) to compare the fluorescent signals between the 5 groups of rats. (B) Representative immunofluorescence images of GFAP (a marker for astrocyte; red) and (C) Iba1 (a marker for microglia; green) labeling in the in the control, SAH24h + Veh, SAH24h + sRAGE, SAH48h + Veh and SAH48h + sRAGE groups (bar = 100 μm). (D) GFAP expression were quantified using the fluorescent intensity (mean gray values in the overall field). (E) The number of Iba1 positive cells was elevated when evaluated at 24 h and 48 h after SAH. Treatment with sRAGE significantly decreased the number of activated microglia compared with SAH + Veh animals. (F) Real-time PCR analysis showed that sRAGE administration reduced the mRNA expression of pro-inflammatory factors, IL-6 and IL-1β in the cortical tissue. Data are expressed as means ± SD.*$P < 0.05$, **$P < 0.01$, ***$P < 0.001$ ($n = 5$ in each group).

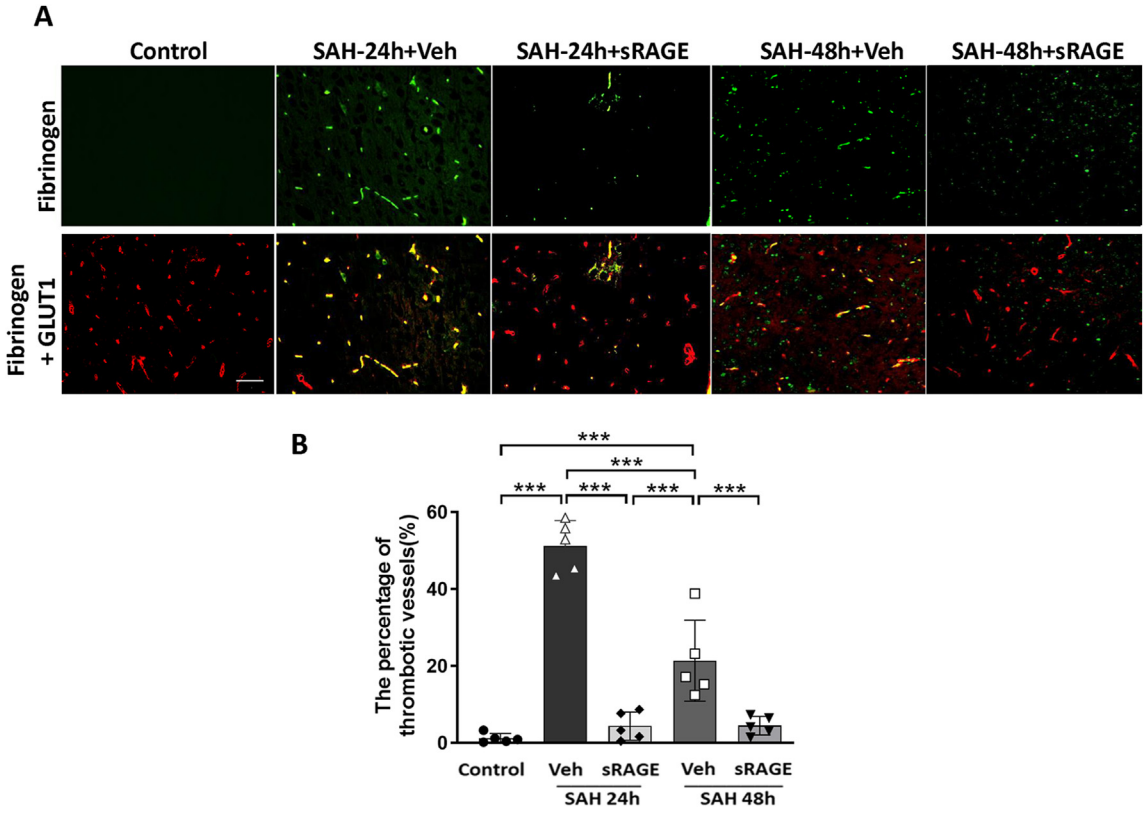

Fig. 5. The number of post-SAH thrombotic vessels was attenuated in the cortex of rats treated with sRAGE. (A) Immunofluorescent images showing fibrinogen (a marker of thrombosis; green) and GLUT1 (a marker of microvessels; red) in the cortical region from the control, SAH24h + Veh, SAH24h + sRAGE, SAH48h + Veh and SAH48h+sRAGE groups. Fibrinogen$^+$ thrombi were detected in the microvessels of the brain parenchyma in the SAH24h+Veh and SAH48h + Veh groups, but were both markedly decreased in the sRAGE groups at 24 and 48 h post-SAH. (B) The percentage of fibrinogen-positive vessels (yellow) was quantified and expressed as mean ± SD. ***$P < 0.001$, $n = 5$ in each group. Bar = 50 μm.

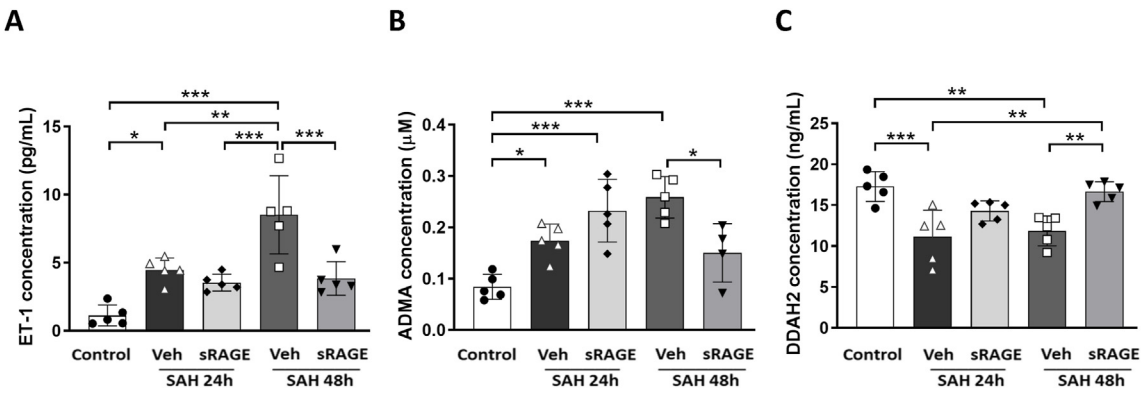

Fig. 6. Effects of sRAGE on endothelial dysfunction at 24 h and 48 h after SAH. Levels of (A) ET-1, (B) ADMA and (C) DDAH2 in rat CSF were measured by ELISA. Treatment with sRAGE significantly decreased the levels of ET-1 and ADMA, and increased DDAH2 as compared with the SAH48h + Veh group. Data are expressed as means ± SD. $^{*}P < 0.05$, $^{**}P < 0.01$, $^{***}P < 0.001$ (n = 4–5 in each group, one data in analysis of ADMA levels had to be excluded due to out of the measurement range).

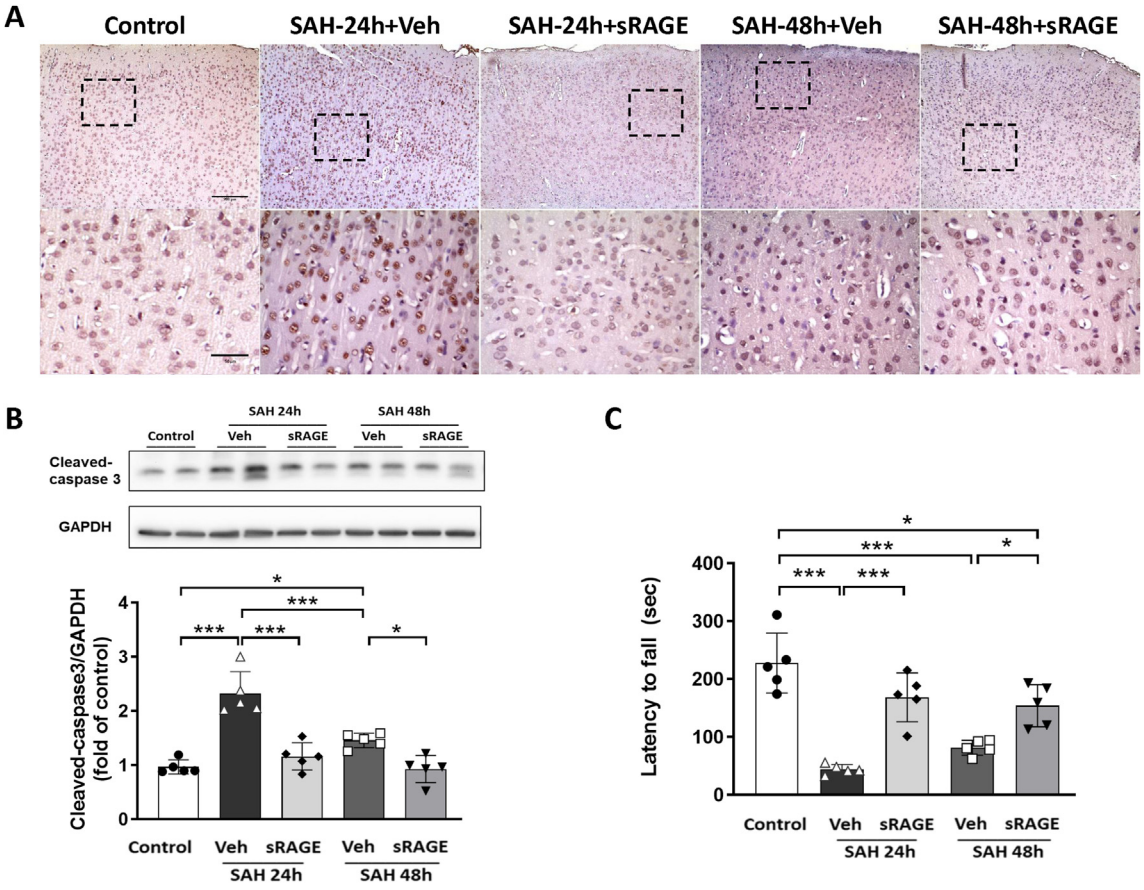

Fig. 7. Administration of sRAGE decreased cellular apoptosis and improved motor function at 24 h and 48 h after SAH. (A) Coronal brain sections were subjected to TUNEL staining in the cortical region of the rats of the control, SAH24h + Veh, SAH24h + sRAGE, SAH48h + Veh and SAH48h + sRAGE groups. The lower panel is an enlargement of boxed areas in the upper panel. Bar = 200 μm (upper panel) and 50 μm (lower panel). (B) Western blots and quantification showed that SAH-induced cleaved caspase-3 was attenuated by sRAGE treatment at both 24 and 48 h after SAH induction. (C) Treatment with sRAGE significantly improved latency to fall as measured by the rotarod test at both 24 and 48 h after SAH induction. Data are expressed as means ± SD. $^{*}P < 0.05$, $^{**}P < 0.01$, $^{***}P < 0.001$ ($n = 5$ in each group).

(p-eNOS) at ser1177, which has been shown to play a crucial role in regulating eNOS activity and promoting NO production [37], at various treatment durations. The WB data showed that expression of p-eNOS exhibited a significant decrease at 12 h within the SAH patient's CSF treatment group when compared to the control group (Fig. 9A). Consequently, this 12-h time point was identified as the optimal treatment duration for HBMECs. Thrombin induces F-actin stress fiber formation in cerebral endothelial cells after hemorrhagic and ischemic stroke, which could be reversed by elevated NO production [38]. The results of double immunofluorescence staining demonstrated that the groups treated with glia-conditioned medium or SAH patient's CSF markedly induced the formation of F-actin stress fibers (visualized using phalloidin staining)

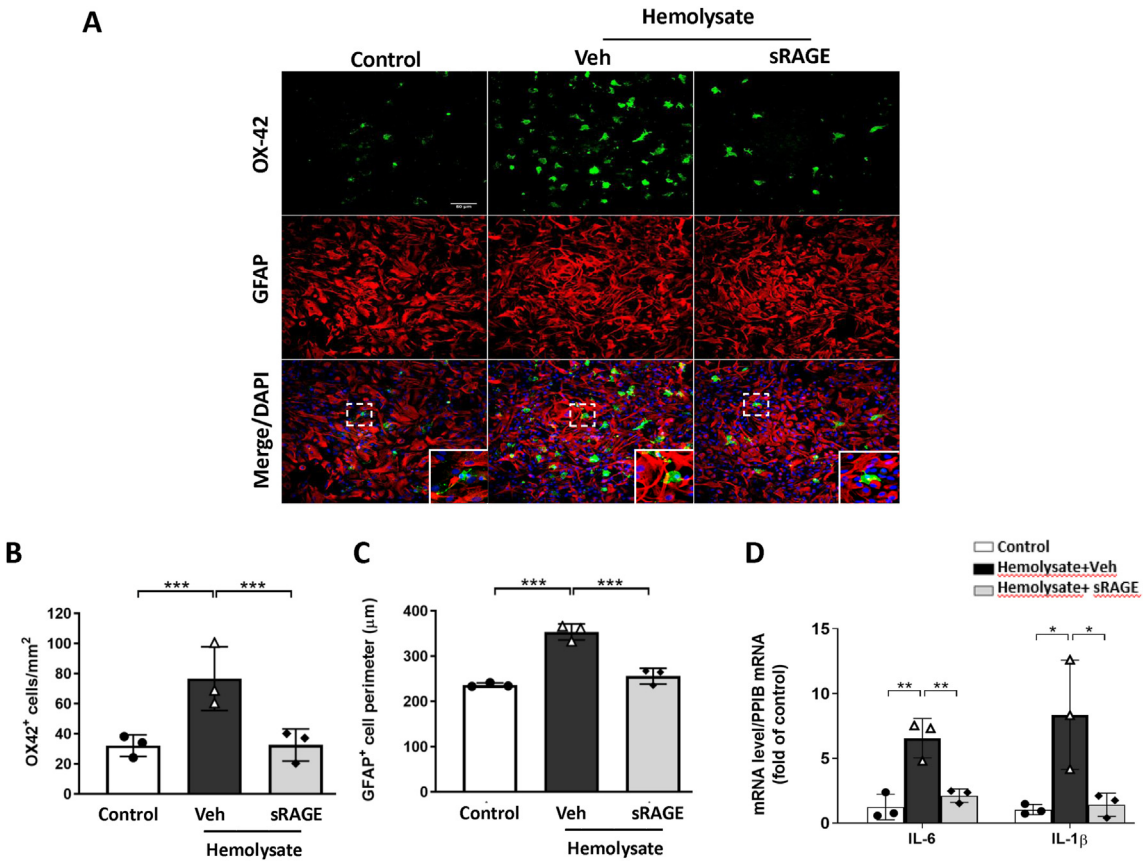

Fig. 8. Treatment with sRAGE reduced microglia activation, astrocyte swelling and pro-inflammatory cytokine mRNA levels in astrocyte–microglia co-cultures exposed to hemolysate. (A) Representative immunofluorescence images of OX42 and GFAP labeling in co-cultures exposed to hemolysate after 24 h. OX42 (a marker for activated microglia) immunoreactivity is shown in green, and GFAP (an astrocyte marker) is shown in red. Bar = 50 μm. Quantitative comparison of (B) OX42-positive cells and (C) GFAP-positive cell perimeter in control, hemolysate-treated with vehicle and sRAGE groups. Real-time PCR analysis showed that sRAGE treatment markedly inhibited (D) IL-6 and IL-1β mRNA levels at 6 h after exposure to hemolysate. Data are expressed as means ± SD. $^{*}P < 0.05$, $^{**}P < 0.01$, $^{***}P < 0.001$ ($n = 3$ in each group).

and the level of p-eNOS were decreased compared with the control group at 12 h in HBMECs (Fig. 9B). However, the stress fiber formation and p-eNOS expression was reversed by treatment with sRAGE. In addition, the WB analysis showed that both the glia-conditioned medium or SAH patient's CSF treated group significantly downregulated p-eNOS expression ($P < 0.001$ and $P < 0.01$ vs. Control, respectively; Fig. 9C&D) and inversely upregulated cleaved caspase3 expression ($P < 0.01$ and $P < 0.001$ vs. Control, respectively; Fig. 9C&F) in the HBMECs. Notably, sRAGE increased the expression of both p-eNOS and eNOS, and attenuated the expression of cleaved caspase-3, as compared with the veh groups in HBMECs (Fig. 9C-F).

Discussion

This study demonstrated that intrathecal administration of recombinant sRAGE attenuated microcirculation impairment and endothelial dysfunction in a rodent model of SAH. By preserving endothelial function after SAH, recombinant sRAGE also reduced astrocyte swelling and thrombosed vessels, thereby prevented neuronal death and improving motor dysfunction in the early phase of experimental SAH. The main protective mechanism of recombinant sRAGE may be mediated via anti-inflammation properties, as revealed in the in vitro model of SAH. We observed reductions in microglia activation and astrocyte swelling, and downregulation of pro-inflammatory cytokine expressions in a primary mixed astrocyte and microglia co-culture treated with hemolysate.

RAGE is a multiligand receptor that can magnify the stress response and contribute to neuroinflammation in various brain insults [39,40]. Among most RAGE ligands, HMGB1 has been proposed to initiate the immune response and may act as a critical contributor to the neuroinflammation underlying SAH [41]. Our previous study demonstrated that the level of CSF HMGB1 in patients with SAH can be a prognostic indicator, and recombinant sRAGE significantly protected against SAH-induced neuronal death in a rat model of SAH [21]. Additionally, we and others have also demonstrated that RAGE inhibition by an antagonist or recombinant sRAGE effectively protects neurons [42] or endothelial cell [43] apoptosis from ischemic reperfusion injury through a mechanism involving reduced HMGB1-RAGE-mediated inflammatory signaling. In the present study, we not only revealed a previously unexplored role of sRAGE in SAH-induced microcirculation impairment, brain edema, astrocyte/microglia activation and endothelial dysfunction, but also demonstrated that sRAGE attenuates markedly increased pro-inflammatory cytokine expressions in vivo and primary mixed astrocyte/microglia co-cultures treated with hemolysate, indicating the crucial pathogenic roles of RAGE-mediated inflammatory responses in SAH.

In our study, the diameters of the sa and ta on the brain surface were significantly increased at 48 h as compared with 24 h post-SAH (Fig. 1C); however, microcirculation impairment, as revealed by the cerebral blood flow and oxygen partial pressure, was not restored at 2 mm underneath the cerebral cortex after 48 h post-SAH (Fig. 2B&C). This phenomenon might be caused by increases in swollen astrocytic end-feet compressing the microvessels underneath the cerebral cortex until 48 h, suggesting that astrocyte swelling contributes largely to the microcirculation impairment. Furthermore, previous studies showed that the neuroinflammatory response may initiate astrocyte swelling rapidly after acute

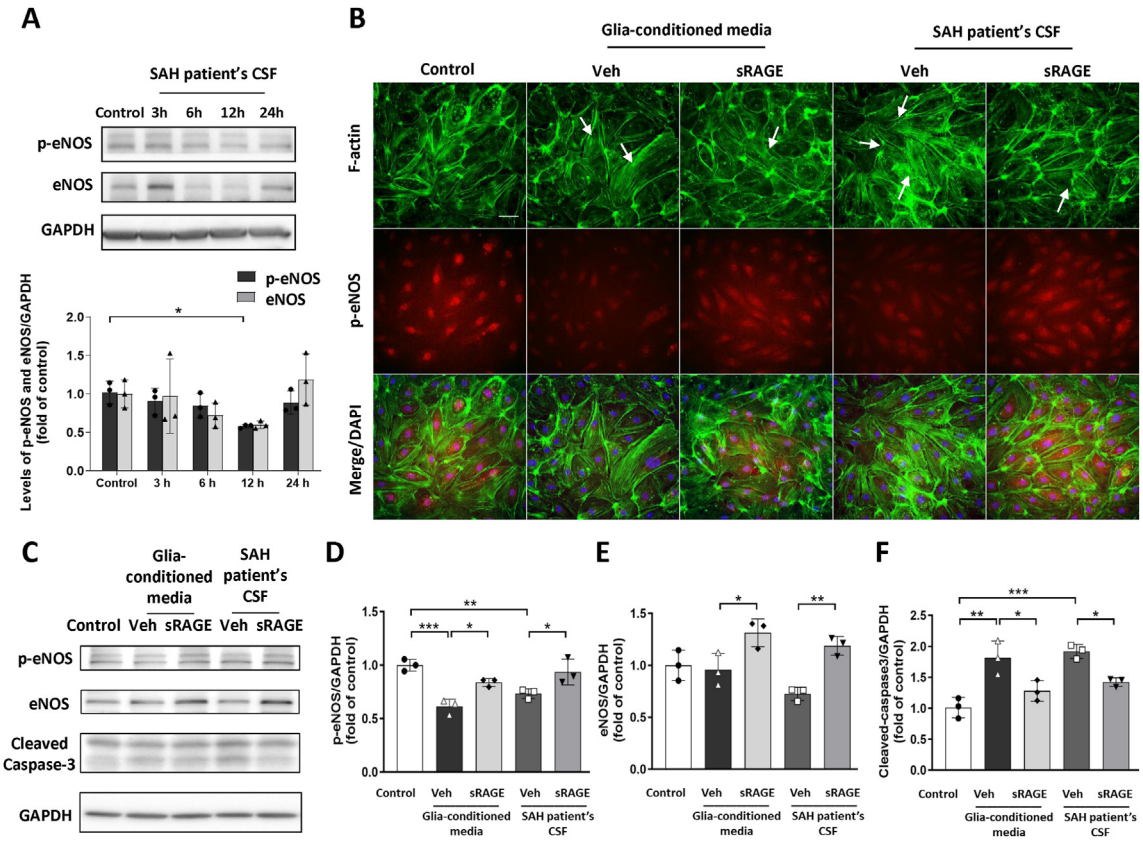

Fig. 9. Recombinant sRAGE increased p-eNOS expression and decreased F-actin formation in HBMECs exposed to glia-conditioned media or SAH-patient's CSF. (A) Time course of p-eNOS (ser1177) and eNOS protein expression by Western immunoblot in HBMECs exposed to 10 % SAH-patient's CSF. The p-eNOS and eNOS protein levels are normalized to GAPDH loading control. (B) Representative immunofluorescence images of F-actin (green, visualized with phalloidin staining) and p-eNOS (red) in HBMECs and stimulated with glia-conditioned media or SAH-patient's CSF for 12 h. Arrows indicate stress fibers formed. Bar = 50 μm. (C) Immunoblot detection and quantification of (D) p-eNOS (ser1177), (E) eNOS, (F) cleaved-caspase3 and GAPDH in HBMECs treated with sRAGE for 12 h. The levels of p-eNOS (Ser 1177) and eNOS were increased and cleaved caspase-3 was attenuated in the presence of sRAGE in HBMECs exposed to glia-conditioned media or SAH-patient's CSF. Expression for each sample was normalized with corresponding GAPDH level. Data are expressed as means ± SD. $^{*}P < 0.05$, $^{**}P < 0.01$, $^{***}P < 0.001$ ($n = 3$ in each group).

SAH and lead to brain edema, which is known to be associated with a poor functional outcome [44,45]. Our results also showed that intrathecal injection of recombinant sRAGE prevented swelling of the astrocytic end-feet post-SAH and further improved the microcirculation and motor function at 24 h and until 48 h post-SAH. Nevertheless, further research is needed to investigate the effect of recombinant sRAGE on SAH-induced BBB disruption. Endothelial dysfunction after SAH causes microcirculation impairment, leading to the occurrence of cerebral vasospasm and cerebral ischemia [46]. This might be another pathology affecting microcirculation impairment at 48 h post-SAH, despite the increased diameters of the sa and ta on the brain surface in the rat model of SAH. Accumulation of ADMA in the CSF could trigger a reduction of endothelium-derived NO production, the most active vasodilator, concurrently with the development of cerebral vasospasm after SAH [34,47]. In contrast, upregulated DDAH enzymatic activity reduces the ADMA expression and stimulates NO production [47]. Several studies have demonstrated that the oxidative stress induced by SAH would decrease the DDAH activity in the CSF and NO availability in the cerebral conductive arteries, which might further result in vasospasm and increase the risk of functional disability and death [48–50]. In the present study, recombinant sRAGE treatment significantly decreased ADMA and increased the DDAH level at 48 h post-SAH, suggesting that recombinant sRAGE might improve NO production and further restore the microcirculation impairment.

Clinical studies have demonstrated that microthrombosis is highly correlated with vasoconstriction following SAH [51–53]. In our study, we found that sRAGE treatment markedly reduced fibrin deposition in the capillaries of the subcortical area at 24 h post-SAH. However, changes in ET-1/NO production were notably observed at 48 h post-SAH, suggesting that sRAGE may involve in multiple mechanisms in ameliorating microthrombosis. In the process of thrombosis, platelets play a pivotal role in blood clot formation, particularly the RAGE receptor is also present on the platelet membrane [54]. Binding of HMGB1 to activated platelets via RAGE contributing to fibrinogen formation, as the ultimate product of the coagulation cascade, leads to stress fiber formation and also initiate localized vasoconstriction to reduce blood flow through the damaged region [55–57]. The mechanisms of sRAGE treatment on microthrombosis after SAH might not only involved in regulating ET-1/NO production, but also in directly blocking platelets activation. Future research is needed to address the multiple protective mechanisms by sRAGE treatment. Together, the early endothelial dysfunction that causes the microcirculation impairment may serve as an initiation for a vicious cycle in which delayed cerebral vasospasm is further triggered, eventually culminating in progressive irreversible tissue damage. By restoring early endothelial function after SAH, recombinant sRAGE may prevent microcirculation impairment and related secondary brain injury.

There were several limitations of this study. First, recombinant sRAGE was administered at the time of SAH induction, as intrathcal injections of autologous blood for SAH induction might increase the intracranial pressure (ICP), and thus intrathecal injection of a sufficient amount of sRAGE would be technically difficult at different time points after SAH. Accordingly, future research is needed to further validate the

efficacy of recombinant sRAGE in an optimal therapeutic time window and via other injection methods (e.g., intraperitoneal or intravenous injections) for clinical application. Second, NO production involves complex interactions among a variety of molecules, and the upregulation of eNOS might not completely determine the level of NO production, which should be explored in the future. Also, recombinant sRAGE underlying the RAGE ligands/RAGE/NF-κB pathway signaling-mediated anti-inflammation requires further investigation. Finally, as this study was limited to pure bench work, further validation is needed to complete a clinical evaluation of CSF components in SAH patients.

In conclusion, the present study demonstrated profound microcirculation restoration and endothelium protection by recombinant sRAGE against SAH brain injury. Recombinant sRAGE could be further explored as a novel therapeutic strategy for SAH.

Author Contributions

Ling-Yu Yang, PhD: Drafting of the manuscript, major role in the acquisition of data, conception and design of study. **Sung-Chun Tang, MD, PhD**: Drafting of the manuscript, major role in the acquisition of data, conception and design of study. **Jing-Er Lee, MD, PhD**: Contributed to the conception of the research and interpretation and analysis of data. **Yong-Ren Chen, MD, PhD**: Contributed to the conception of the research and interpretation and analysis of data. **Yi-Tzu Chen, MS**: Contributed to the conception of the research, performed experiments and analysis of data. **Kuo-Wei Chen, MD**: Contributed to the conception of the research. **Sung-Tsang Hsieh, MD, PhD**: Contributed to the conception of the research. **Kuo-Chuan Wang** MD, PhD: Drafting of the manuscript, major role in the acquisition of data, conception and design of study.

Funding

This research was funded by the Ministry of Science and Technology, Taiwan (MOST108-2314-B-002-085-MY2, MOST110-2314-B-002-159 and MOST111-2314-B-002-254-MY2).

Declaration of competing interest

The authors declare the following financial interests/personal relationships which may be considered as potential competing interests: Kuo-Chuan Wang reports financial support was provided by Ministry of Science and Technology, Taiwan. If there are other authors, they declare that they have no known competing financial interests or personal relationships that could have appeared to influence the work reported in this paper.

Acknowledgments

This work was supported in part by the 2nd and 3rd Core Facility and Animal Core Facility, Department of Medical Research, at National Taiwan University Hospital.

References

[1] Schievink WI. Intracranial aneurysms. N Engl J Med 1997;336(1):28–40.
[2] Suarez JI, Tarr RW, Selman WR. Aneurysmal subarachnoid hemorrhage. N Engl J Med 2006;354(4):387–96.
[3] Broderick JP, Brott TG, Duldner JE, Tomsick T, Leach A. Initial and recurrent bleeding are the major causes of death following subarachnoid hemorrhage. Stroke 1994;25(7):1342–7.
[4] Sehba FA, Pluta RM, Zhang JH. Metamorphosis of subarachnoid hemorrhage research: from delayed vasospasm to early brain injury. Mol Neurobiol 2011;43(1):27–40.
[5] Ohkuma H, Itoh K, Shibata S, Suzuki S. Morphological changes of intraparenchymal arterioles after experimental subarachnoid hemorrhage in dogs. Neurosurgery 1997;41(1):230–5. discussion 235-236.
[6] Sun BL, Zheng CB, Yang MF, Yuan H, Zhang SM, Wang LX. Dynamic alterations of cerebral pial microcirculation during experimental subarachnoid hemorrhage. Cell Mol Neurobiol 2009;29(2):235–41.
[7] Pardridge WM. The isolated brain microvessel: a versatile experimental model of the blood-brain barrier. Front Physiol 2020;11:398.
[8] Mathiisen TM, Lehre KP, Danbolt NC, Ottersen OP. The perivascular astroglial sheath provides a complete covering of the brain microvessels: an electron microscopic 3D reconstruction. Glia 2010;58(9):1094–103.
[9] Hudetz AG. The cerebral microcirculation in ischemia and hypoxemia. The Arisztid G. B. Kovach Memorial Lecture. Adv Exp Med Biol 2003;530:347–57.
[10] Zlokovic BV. Neurovascular pathways to neurodegeneration in Alzheimer's disease and other disorders. Nat Rev Neurosci 2011;12(12):723–38.
[11] Bierhaus A, Humpert PM, Morcos M, Wendt T, Chavakis T, Arnold B, et al. Understanding RAGE, the receptor for advanced glycation end products. J Mol Med (Berl) 2005;83(11):876–86.
[12] Schmidt AM, Yan SD, Yan SF, Stern DM. The biology of the receptor for advanced glycation end products and its ligands. Biochim Biophys Acta 2000;1498(2–3):99–111.
[13] Goyal M, Menon BK, van Zwam WH, Dippel DW, Mitchell PJ, Demchuk AM, et al. Endovascular thrombectomy after large-vessel ischaemic stroke: a meta-analysis of individual patient data from five randomised trials. Lancet 2016;387(10029):1723–31.
[14] Muhammad S, Barakat W, Stoyanov S, Murikinati S, Yang H, Tracey KJ, et al. The HMGB1 receptor RAGE mediates ischemic brain damage. J Neurosci 2008;28(46):12023–31.
[15] Yang L, Wang F, Yang L, Yuan Y, Chen Y, Zhang G, et al. HMGB1 a-box reverses brain edema and deterioration of neurological function in a traumatic brain injury mouse model. Cell Physiol Biochem 2018;46(6):2532–42.
[16] Wang D, Liu K, Wake H, Teshigawara K, Mori S, Nishibori M. Anti-high mobility group box-1 (HMGB1) antibody inhibits hemorrhage-induced brain injury and improved neurological deficits in rats. Sci Rep 2017;7:46243.
[17] Zhang J, Takahashi HK, Liu K, Wake H, Liu R, Maruo T, et al. Anti-high mobility group box-1 monoclonal antibody protects the blood-brain barrier from ischemia-induced disruption in rats. Stroke 2011;42(5):1420–8.
[18] Li H, Yu JS, Zhang DD, Yang YQ, Huang LT, Yu Z, et al. Inhibition of the receptor for advanced glycation end-products (RAGE) attenuates neuroinflammation while sensitizing cortical neurons towards death in experimental subarachnoid hemorrhage. Mol Neurobiol 2017;54(1):755–67.
[19] Li H, Wu W, Sun Q, Liu M, Li W, Zhang XS, et al. Expression and cell distribution of receptor for advanced glycation end-products in the rat cortex following experimental subarachnoid hemorrhage. Brain Res 2014;1543:315–23.
[20] Herold K, Moser B, Chen Y, Zeng S, Yan SF, Ramasamy R, et al. Receptor for advanced glycation end products (RAGE) in a dash to the rescue: inflammatory signals gone awry in the primal response to stress. J Leukoc Biol 2007;82(2):204–12.
[21] Wang KC, Tang SC, Lee JE, Li YI, Huang YS, Yang WS, et al. Cerebrospinal fluid high mobility group box 1 is associated with neuronal death in subarachnoid hemorrhage. J Cerebr Blood Flow Metabol 2017;37(2):435–43.
[22] Wang KC, Tang SC, Lee JE, Tsai JC, Lai DM, Lin WC, et al. Impaired microcirculation after subarachnoid hemorrhage in an in vivo animal model. Sci Rep 2018;8(1):13315.
[23] Percie du Sert N, Hurst V, Ahluwalia A, Alam S, Avey MT, Baker M, et al. The ARRIVE guidelines 2.0: updated guidelines for reporting animal research. J Cerebr Blood Flow Metabol 2020;40(9):1769–77.
[24] Chen TF, Chen KW, Chien Y, Lai YH, Hsieh ST, Ma HY, et al. Dental pulp stem cell-derived factors alleviate subarachnoid hemorrhage-induced neuroinflammation and ischemic neurological deficits. Int J Mol Sci 2019;20(15).
[25] Suzuki H, Hasegawa Y, Kanamaru K, Zhang JH. Mechanisms of osteopontin-induced stabilization of blood-brain barrier disruption after subarachnoid hemorrhage in rats. Stroke 2010;41(8):1783–90.
[26] Shiotsuki H, Yoshimi K, Shimo Y, Funayama M, Takamatsu Y, Ikeda K, et al. A rotarod test for evaluation of motor skill learning. J Neurosci Methods 2010;189(2):180–5.
[27] Yang LY, Chen YR, Lee JE, Chen KW, Luh HT, Chen YT, et al. Dental pulp stem cell-derived conditioned medium alleviates subarachnoid hemorrhage-induced microcirculation impairment by promoting M2 microglia polarization and reducing astrocyte swelling. Transl Stroke Res 2023;14(5):688–703.
[28] Wang JY, Shum AY, Chao CC, Kuo JS, Wang JY. Production of macrophage inflammatory protein-2 following hypoxia/reoxygenation in glial cells. Glia 2000;32(2):155–64.
[29] Dang B, Shen H, Li H, Zhu M, Guo C, He W. Matrix metalloproteinase 9 may be involved in contraction of vascular smooth muscle cells in an in vitro rat model of subarachnoid hemorrhage. Mol Med Rep 2016;14(5):4279–84.
[30] Nakao VW, Mazucanti CHY, de Sa Lima L, de Mello PS, de Souza Port's NM, Kinoshita PF, et al. Neuroprotective action of alpha-Klotho against LPS-activated glia conditioned medium in primary neuronal culture. Sci Rep 2022;12(1):18884.
[31] Shi Z, Zhang W, Lu Y, Lu Y, Xu L, Fang Q, et al. Aquaporin 4-mediated glutamate-induced astrocyte swelling is partially mediated through metabotropic glutamate receptor 5 activation. Front Cell Neurosci 2017;11:116.
[32] Sorensen AG, Patel S, Harmath C, Bridges S, Synnott J, Sievers A, et al. Comparison of diameter and perimeter methods for tumor volume calculation. J Clin Oncol 2001;19(2):551–7.
[33] Iglarz M, Clozel M. Mechanisms of ET-1-induced endothelial dysfunction. J Cardiovasc Pharmacol 2007;50(6):621–8.
[34] Jung CS, Iuliano BA, Harvey-White J, Espey MG, Oldfield EH, Pluta RM. Association between cerebrospinal fluid levels of asymmetric dimethyl-L-arginine, an

endogenous inhibitor of endothelial nitric oxide synthase, and cerebral vasospasm in a primate model of subarachnoid hemorrhage. J Neurosurg 2004;101(5):836–42.
[35] Salonia R, Empey PE, Poloyac SM, Wisniewski SR, Klamerus M, Ozawa H, et al. Endothelin-1 is increased in cerebrospinal fluid and associated with unfavorable outcomes in children after severe traumatic brain injury. J Neurotrauma 2010; 27(10):1819–25.
[36] Sibal L, Agarwal SC, Home PD, Boger RH. The role of asymmetric dimethylarginine (ADMA) in endothelial dysfunction and cardiovascular disease. Curr Cardiol Rev 2010;6(2):82–90.
[37] Dimmeler S, Fleming I, Fisslthaler B, Hermann C, Busse R, Zeiher AM. Activation of nitric oxide synthase in endothelial cells by Akt-dependent phosphorylation. Nature 1999;399(6736):601–5.
[38] Atkinson L, Yusuf MZ, Aburima A, Ahmed Y, Thomas SG, Naseem KM, et al. Reversal of stress fibre formation by Nitric Oxide mediated RhoA inhibition leads to reduction in the height of preformed thrombi. Sci Rep 2018;8(1):3032.
[39] MacLean M, Derk J, Ruiz HH, Juranek JK, Ramasamy R, Schmidt AM. The Receptor for Advanced Glycation End Products (RAGE) and DIAPH1: implications for vascular and neuroinflammatory dysfunction in disorders of the central nervous system. Neurochem Int 2019;126:154–64.
[40] Vincent AM, Perrone L, Sullivan KA, Backus C, Sastry AM, Lastoskie C, et al. Receptor for advanced glycation end products activation injures primary sensory neurons via oxidative stress. Endocrinology 2007;148(2):548–58.
[41] Sun Q, Wang F, Li W, Li W, Hu YC, Li S, et al. Glycyrrhizic acid confers neuroprotection after subarachnoid hemorrhage via inhibition of high mobility group box-1 protein: a hypothesis for novel therapy of subarachnoid hemorrhage. Med Hypotheses 2013;81(4):681–5.
[42] Tang SC, Wang YC, Li YI, Lin HC, Manzanero S, Hsieh YH, et al. Functional role of soluble receptor for advanced glycation end products in stroke. Arterioscler Thromb Vasc Biol 2013;33(3):585–94.
[43] Mi L, Zhang Y, Xu Y, Zheng X, Zhang X, Wang Z, et al. HMGB1/RAGE pro-inflammatory axis promotes vascular endothelial cell apoptosis in limb ischemia/reperfusion injury. Biomed Pharmacother 2019;116:109005.
[44] Claassen J, Carhuapoma JR, Kreiter KT, Du EY, Connolly ES, Mayer SA. Global cerebral edema after subarachnoid hemorrhage: frequency, predictors, and impact on outcome. Stroke 2002;33(5):1225–32.
[45] Zetterling M, Hallberg L, Ronne-Engstrom E. Early global brain oedema in relation to clinical admission parameters and outcome in patients with aneurysmal subarachnoid haemorrhage. Acta Neurochir (Wien) 2010;152(9):1527–33.
[46] Geraghty JR, Davis JL, Testai FD. Neuroinflammation and microvascular dysfunction after experimental subarachnoid hemorrhage: emerging components of early brain injury related to outcome. Neurocritical Care 2019; 31(2):373–89.
[47] Palm F, Onozato ML, Luo Z, Wilcox CS. Dimethylarginine dimethylaminohydrolase (DDAH): expression, regulation, and function in the cardiovascular and renal systems. Am J Physiol Heart Circ Physiol 2007;293(6):H3227–45.
[48] Pluta RM. Dysfunction of nitric oxide synthases as a cause and therapeutic target in delayed cerebral vasospasm after SAH. Acta Neurochir Suppl 2008;104:139–47.
[49] Nakata S, Tsutsui M, Shimokawa H, Suda O, Morishita T, Shibata K, et al. Spontaneous myocardial infarction in mice lacking all nitric oxide synthase isoforms. Circulation 2008;117(17):2211–23.
[50] Clark JF, Reilly M, Sharp FR. Oxidation of bilirubin produces compounds that cause prolonged vasospasm of rat cerebral vessels: a contributor to subarachnoid hemorrhage-induced vasospasm. J Cerebr Blood Flow Metabol 2002;22(4):472–8.
[51] Suzuki S, Kimura M, Souma M, Ohkima H, Shimizu T, Iwabuchi T. Cerebral microthrombosis in symptomatic cerebral vasospasm–a quantitative histological study in autopsy cases. Neurol Med -Chir 1990;30(5):309–16.
[52] Romano JG, Rabinstein AA, Arheart KL, Nathan S, Campo-Bustillo I, Koch S, et al. Microemboli in aneurysmal subarachnoid hemorrhage. J Neuroimaging 2008; 18(4):396–401.
[53] Stein SC, Browne KD, Chen XH, Smith DH, Graham DI. Thromboembolism and delayed cerebral ischemia after subarachnoid hemorrhage: an autopsy study. Neurosurgery 2006;59(4):781–7.
[54] Ahrens I, Chen YC, Topcic D, Bode M, Haenel D, Hagemeyer CE, et al. HMGB1 binds to activated platelets via the receptor for advanced glycation end products and is present in platelet rich human coronary artery thrombi. Thromb Haemostasis 2015; 114(5):994–1003.
[55] Hou Y, Carrim N, Wang Y, Gallant RC, Marshall A, Ni H. Platelets in hemostasis and thrombosis: novel mechanisms of fibrinogen-independent platelet aggregation and fibronectin-mediated protein wave of hemostasis. J Biomed Res 2015;29(6): 437–44.
[56] Lominadze D, Dean WL, Tyagi SC, Roberts AM. Mechanisms of fibrinogen-induced microvascular dysfunction during cardiovascular disease. Acta Physiol 2010; 198(1):1–13.
[57] Vogel S, Bodenstein R, Chen Q, Feil S, Feil R, Rheinlaender J, et al. Platelet-derived HMGB1 is a critical mediator of thrombosis. J Clin Invest 2015;125(12):4638–54.